

A linearized theory of transient laser heating in fluids

R. Holmes

Rockwell International Corporation, Rocketdyne Division, 6633 Canoga Avenue, Mailstop FA40, Canoga Park, California 91303

R. Myers and C. Duzy

North East Research Associates, 800 West Cummings Park, Suite 4900, Woburn, Massachusetts 02181

(Received 14 January 1991)

A linear theory of laser heating is used to describe the coupling of optical waves to thermally induced acoustic and entropy perturbations of the medium. The analysis differs from those of previous authors in its treatment of entropy, dissipative effects, and active compensation of thermally induced laser-beam aberrations. An intuitively simple equation for the medium perturbation is derived, within the hydrodynamic approximation. The dimensionless parameters that characterize the diverse scattering regimes are discussed. The boundary-value problem is solved for specific cases of interest. Comparison with a nonlinear simulation verifies the linearized result in such cases.

PACS number(s): 42.68.Mj, 42.20.Ji, 42.65.Es, 62.60.+v

I. INTRODUCTION

In a number of applications, a laser-beam pulse propagates through an absorbing fluid. Such applications include transmission of lasers through the atmosphere. The fraction of energy lost to the medium might be a relatively small portion of the total energy, yet sufficient to disturb the medium, creating acoustic waves that may move a significant distance transverse to the propagation direction during the pulse. Such waves lead to the well-known t^3 -blooming refractive-index variations [1,2]. As the medium attains mechanical equilibrium, a linear time dependence is found—this is referred to as steady-state thermal blooming. When such blooming is sufficiently strong, the induced refractive index alters the intensity profile of the beam further along the propagation path. This altered intensity profile induces a somewhat different refractive-index profile that may reinforce the path-integrated t^3 or t^1 blooming. This self-enhancement may be called stimulated thermal Brillouin scattering or stimulated thermal Rayleigh scattering, respectively [3]. In principle, this scattering may occur in any direction. In practice, the greatest enhancement occurs in the near-forward or near-backward direction, because these directions have the greatest overlap with the scattering beam. Such scattering may be analyzed using a linearized theory; the linearized theory has been relatively successful in predicting behavior for steady-state thermal blooming and is anticipated to be so in this case also, provided the heating-induced aberrations do not remove a substantial portion of the beam energy [4,5]. Thus this approach neglects important nonlinear effects such as laser depletion [6] and absorber saturation. On the other hand, many treatments use a linearized theory, including some of the earliest works in laser heating [3,7–9]. Since those earliest efforts, the approach has been refined repeatedly to include the effects of high spatial frequencies [10,11], resonant absorption and emission [12], compensation of both phase and intensity [13–15], and instability-growth

effects [14–16]. A key realization in much of the latest work involves the effect of medium turbulence. Turbulence-induced refractive-index variations have been known and studied extensively [17]. However, only recently has it been discovered that turbulence-induced scintillation creates substantial local-heating variations in cases of interest [4,10,13,16]. The scintillation effects are naturally treated through the Rytov approximation, which utilizes the phase and log-amplitude as the dependent variables [17]. Within this formalism, the important four-photon processes of stimulated thermal scattering, first treated by Kroll and Kelley [9], are included in some of the more recent works [4]. This formalism predicts that the phase diffracts into intensity variations that form a seed for an effect that is now known as near-forward stimulated thermal Rayleigh scattering STRS [3]. This effect has also been referred to as thermally amplified scintillation (TAS), or as a turbulence-thermal-blooming interaction (TTBI) [4,13,14,18]. STRS occurs when the laser-beam-heated region has attained mechanical equilibrium with the surrounding medium. Thus the heated regions are at a different density and temperature—the entropy of the medium is a function of position, one which oscillates and grows. This solution may be thought of as an entropy fluctuation of the medium coupled to a spatial perturbation of the optical field.

The effect of localized scintillation may also be significant within a pulse, especially for high-intensity pulses with pulse durations in excess of a few microseconds [19]. In this early-time regime, Brillouin scattering by thermally induced acoustic waves may result in what is known as stimulated thermal Brillouin scattering (STBS) [3]. In this case, the density fluctuations associated with acoustic waves are what couple to a perturbation of the optical field. Our principal aim in this work is to extend existing linearized theories to treat the acoustic-optical modes of near-forward STBS. The following section outlines a derivation of these equations convenient for accomplishment of this aim.

II. BASIC EQUATIONS

The basic equations of motion for a simple fluid are given by expressions for the conservation of mass, momentum, and energy:

$$\partial_t \rho + \sum_j \frac{\partial}{\partial x_j} (\rho v_j) = 0, \quad (1)$$

$$\partial_t \rho v_i + \sum_j \frac{\partial}{\partial x_j} (\rho v_i v_j + P \delta_{ij} - \sigma_{ji}) = 0, \quad i = 1, 2, 3 \quad (2)$$

$$\begin{aligned} \partial_t \rho \left[u + \frac{v^2}{2} \right] \\ + \sum_j \frac{\partial}{\partial x_j} \left\{ \left[\rho \left[u + \frac{v^2}{2} \right] + P \right] v_j \right. \\ \left. - \sum_i \sigma_{ji} v_i - \kappa_T \frac{\partial T}{\partial x_j} \right\} = \dot{q}, \end{aligned} \quad (3)$$

where ρ , u , P , \mathbf{v} , and T are the density, internal energy per unit mass, pressure, velocity, and temperature, respectively, of the medium, and \dot{q} is the rate of heat added per unit volume. The mass flux $\rho \mathbf{v}$ is the sum of the kinematic mass flux and the flux arising from diffusion of density variations:

$$\rho \mathbf{v} = \rho \mathbf{v}' - \kappa_D \nabla \rho, \quad (4)$$

where κ_D is the self-diffusion constant. In addition to diffusion, the dissipative effects of thermal conductivity and viscosity are included. The thermal conductivity is given by $\kappa_T = c_p \eta / \mathcal{P} \equiv c_v \eta / \lambda$, where \mathcal{P} is the Prandtl number of the medium, $c_{p,v}$ are the specific heats per unit mass, and η is the coefficient of first viscosity. Viscosity is explicitly included through the viscous stress tensor σ_{ij}

$$\sigma_{ij} = \eta \left[\frac{\partial v_i}{\partial x_j} + \frac{\partial v_j}{\partial x_i} - \frac{2}{3} \delta_{ij} \nabla \cdot \mathbf{v} \right] + \zeta \nabla \cdot \mathbf{v}, \quad (5)$$

where ζ is the coefficient of second viscosity. This neglects the well-known relaxation effects that occur outside the hydrodynamic approximation [20].

In Eqs. (1)–(3), there are seven dependent variables, including the three components of velocity. Thus a minimum of two more equations are needed. If the entropy s per unit mass is introduced, then three more equations are needed. As is well known, the set of four thermodynamic quantities (ρ, P, T, s) are not independent; any pair may be expressed as a function of the remaining pair for a simple fluid. Thus we may choose to eliminate the pair (P, T) in favor of (ρ, s). These relations may be expressed in differential form for our purposes. Thus, in differential form, with the derivatives assumed given,

$$\delta T = \left[\frac{\partial T}{\partial \rho} \right]_s \delta \rho + \left[\frac{\partial T}{\partial s} \right]_\rho \delta s, \quad (6)$$

$$\delta P = \left[\frac{\partial P}{\partial \rho} \right]_s \delta \rho + \left[\frac{\partial P}{\partial s} \right]_\rho \delta s, \quad (7)$$

where $(\partial P / \partial s)_\rho = \rho^2 (\partial T / \partial \rho)_s$ from the Maxwell-Gibbs relations, $(\partial P / \partial \rho)_s = v_0^2$ for the limit of small density perturbations, v_0 is the acoustic velocity, $(\partial T / \partial s)_\rho = T / c_v$, and c_v is the specific heat per unit mass. The simple expressions (6) and (7) become more complicated when temporal and spatial variations of the medium occur on scales of the mean free time or mean free path, respectively, i.e., when local thermodynamic equilibrium is not obtained. These complications will be neglected. To the above equations the energy equation may be added, to provide the final needed equation. Here again, the differential form is adequate:

$$\delta u = (P / \rho^2) \delta \rho + T \delta s. \quad (8)$$

The remaining partial derivative $\rho^2 (\partial T / \partial \rho)_s$ may be evaluated easily in terms of basic experimental parameters using well-known thermodynamic relations to yield

$$\rho^2 \left[\frac{\partial T}{\partial \rho} \right]_s = (\alpha_e / c_p) v_0^2 \rho T = \alpha_e T / \beta_T c_v = (\gamma - 1) \rho T, \quad (9)$$

where the last equality holds for the case of an ideal gas, γ is the ratio of specific heats, and where α_e and β_T are the isobaric coefficient of thermal expansion and the isothermal coefficient of compressibility, respectively.

The above equations are linearized about spatially and temporally homogeneous zeroth-order values of the dependent variables,

$$\rho = \rho_0 + \delta \rho, \quad (10a)$$

$$s = s_0 + \delta s, \quad (10b)$$

$$\mathbf{v} = \mathbf{v}_0 + \delta \mathbf{v}. \quad (10c)$$

A further simplification results by setting \mathbf{v}_0 to zero—this may be done without loss of generality because the conservation equations are invariant under Galilean transformations. A simple change of variables, $\mathbf{x}_1 = \mathbf{x} - \mathbf{v}_0 t$, reduces the more complicated case to the simpler case. To complete the development, the laser-induced heating must be introduced. The laser typically excites an internal degree of freedom of the molecules that compose the fluid. The result is a nonequilibrium population shift n_1 of molecules into an excited state of energy ΔE , which energy is some fraction of the quantum of laser energy $h\nu$. The energy ΔE contained in this mode then relaxes into translational energy, i.e., heat, through an exponential process with decay rate Γ . The remaining photon energy is removed through nonthermal mechanisms. Thus, assuming a two-state system with total population n_{01} ,

$$\dot{q} = \Delta E \Gamma n_1, \quad (11)$$

$$(\partial_t + \Gamma) n_1 = (\alpha' / h\nu) I (1 - 2n_1 / n_{01}), \quad (12a)$$

where α' is the photon absorption per cm. An expression equivalent to Eq. (12a) may be written for the heating rate; defining a normalized absorption per cm, $\alpha = \alpha' \Delta E / h\nu$, and neglecting population saturation effects, one has

$$(\partial_t + \Gamma)\dot{q} = \alpha\Gamma I . \tag{12b}$$

In general, the decay rate Γ depends on both the population decay rate and the diffusion of stored internal energy [6,21,22]. Typically, however, the relaxation rate is dominated by the two-level population decay rate, equal to the inverse of the T_2 decay time [22]. This is especially true for forward scattering, for which the low spatial frequencies involved imply that diffusion occurs on a relatively long time scale.

One may now proceed to combine Eq. (12b) with the linearized versions of Eqs. (1)–(3) which then yields the following result [23]:

$$\frac{\partial\delta\rho}{\partial t} + \rho_0\nabla\cdot\delta\mathbf{v} = 0 , \tag{13}$$

$$\rho_0\frac{\partial\delta\mathbf{v}}{\partial t} = -v_0^2\nabla\delta\rho - \rho_0^2\left[\frac{\partial T}{\partial\rho}\right]_s\nabla\delta s + \eta\nabla^2\delta\mathbf{v} + (\zeta + \eta/3)\nabla(\nabla\cdot\delta\mathbf{v}) , \tag{14}$$

$$\left[\frac{\partial}{\partial t} + \Gamma\right]\rho_0\left[T_0\left[\frac{\partial}{\partial t} - \frac{\kappa_T}{c_v\rho_0}\nabla^2\right]\delta s - \frac{\kappa_T}{\rho_0}\left[\frac{\partial T}{\partial\rho}\right]_s\nabla^2\delta\rho\right] = \alpha\Gamma I . \tag{15}$$

These equations may be simplified yet further by eliminating the velocity perturbation. This is accomplished by taking the divergence of Eq. (14) and using Eq. (13) in the reduced equation to substitute the density for the divergence of the velocity perturbation. Equation (14) is reduced to an expression involving the density and entropy only. This last reduction obviously only accounts for

the effect of the divergence of the velocity. On the other hand, the Stokes-Helmholtz theorem states that the velocity field can be decomposed into two fields—a curl-free component with nonzero divergence, and a divergence-free component with nonzero curl. The former component is accounted for in the expressions for s and ρ ; the latter component is not. One finds that the latter component makes no contribution provided the laser intensity introduces only curl-free forces in Eqs. (14). In the simple case of laser heating, the laser beam provides negligible direct force; thus it is seen that the curl of the velocity makes no contribution.

Of the two remaining equations, one may be eliminated in favor of the other. Choosing the density because it is most relevant for heating-induced laser aberrations, one obtains the relatively transparent expression

$$[\partial_{t_1}^2 - v_0^2\nabla^2 - \eta_0(\frac{4}{3} + r)\partial_{t_1}\nabla^2][\partial_{t_1} - (\eta_0/\mu)\nabla^2](\partial_{t_1} + \Gamma)\delta\rho = \alpha\Psi\Gamma\nabla^2 I + c_v T_0\Psi^2(\eta_0/\mu)\nabla^2\nabla^2(\partial_{t_1} + \Gamma)\delta\rho , \tag{16a}$$

where $\Psi = (\partial T/\partial\rho)_s(\rho_0/T_0)$, $\eta_0 = \eta/\rho_0$ is the kinematic first (shear) viscosity, and r is the ratio of the second viscosity to first viscosity. t_1 is the convection time in the convected frame, so that

$$\partial_{t_1} = \partial_t - \mathbf{v}(z)\cdot\nabla ,$$

where $\mathbf{v}(z)$ is the medium flow velocity, a function of position along the laser-beam propagation path. With smooth variations of the flow along the optical propagation path, Eq. (16a) retains its validity [1,2], and this variable-wind case is included in the formalism. The above equation for density variation is supplemented with a similar equation for the entropy perturbation s:

$$[\partial_{t_1}^2 - v_0^2\nabla^2 - \eta_0(\frac{4}{3} + r)\partial_{t_1}\nabla^2][\partial_{t_1} - (\eta_0/\mu)\nabla^2](\partial_{t_1} + \Gamma)\delta s = [\partial_{t_1}^2 - v_0^2\nabla^2 - \eta_0(\frac{4}{3} + r)\partial_{t_1}\nabla^2]\left[\frac{\alpha\Gamma}{\rho_0 T_0}\right]\nabla^2 I + c_v T_0\Psi^2(\eta_0/\mu)\nabla^2\nabla^2(\partial_{t_1} + \Gamma)\delta s . \tag{16b}$$

These are our basic equations for transient laser heating.

This latter equation differs from the previous one only in that the differential operator on the optical intensity takes a wavelike form. These equations for the density and entropy then form a complete description of the response of the medium to heat deposition by optical waves within the linearized hydrodynamic approximation. In the opinion of the authors, these equations are more obvious than earlier descriptions that involve temperature rather than entropy.

It can be seen that the dissipative terms typically involve powers of the Laplacian operator; this implies that dissipative effects are especially important for finer-scale perturbations. These effects tend to damp the high-spatial frequency perturbations that would otherwise dominate the results obtained from solution of previous approximations [1,2]. The above equation correctly generalizes the sound velocity to include the transition from

adiabatic to isothermal compression that occurs for the higher-spatial frequencies. The simple t^3 regime is recovered by the neglect of all terms involving the Laplacian of the density perturbation and by assuming the population decay is in steady state.

The above equation has a form amenable to simple explanation. The differential operator is factored into three operators, one of which has wavelike solutions; the second has diffusive solutions; the third corresponds to decay of the excited-state population. An additional term on the right-hand sides of Eqs. (16) is present to account for the effect of entropy-density coupling at higher spatial frequencies. The wavelike solutions move with the acoustic velocity and correspond to sound waves damped by viscous forces. As these waves progress, they move out from the heated regions, “uncovering” a heated slug of the medium that is in mechanical equilibrium with the cooler surrounding gas. This slug may have variations in

entropy according to variations in heat deposition. Such variations decay through thermal conduction. When the source of heat deposition, e.g., a laser beam, is altered by these variations, these perturbing variations will oscillate and grow, both temporally and spatially [9]. This may be seen from Eqs. (47)–(50); perturbations of the laser beam grow concurrently as may be seen from Eqs. (52). These perturbations of the laser beam are distortions that arise from the spatially varying heat content of the medium. As mentioned earlier, this particular type of scattering is named stimulated thermal Rayleigh scattering [3].

In addition to scattering from entropy waves, scattering may also occur from the previously mentioned acoustic waves. This analysis breaks naturally into two separate cases—near-forward and near-backward STBS. Scattering angles that are neither near forward nor near backward are of less interest—such large-angle scattering typically leaves the irradiated volume before it is enhanced by further interaction. The backward-scattering case is of some interest when the laser coherence length is sufficiently long—this case is treated in the Sec. III. Our main interest is in near-forward scattering; thus the remainder of the paper will be devoted to that case.

Near-forward STBS or STRS is often described as thermal blooming. An important simplification occurs in such instances—the variations of the envelope of the electric field and the density perturbations parallel to the propagation axis are much smaller than those perpendicular to the propagation axis: The ratio of the derivative parallel to the axis $\partial_z E$ to that perpendicular to the axis $\nabla_\perp E$ is approximately equal to λ/D_\perp , where λ is the spatial period of the perturbation, and D_\perp is the optical wavelength. Thus the z derivatives of the density and entropy are neglected. Another relevant simplification is the assumption that the fluid is an ideal gas. For an ideal gas, one may use Eq. (9) to simplify Eqs. (16). One finds that $\Psi = (\gamma - 1)$, and that $c_v T_0 \Psi^2 = [(\gamma - 1)/\gamma] v_0^2$. A third assumption that is often appropriate is that the population transfer has reached a steady state; often the population decay rate is on the order of nanoseconds, during which time the acoustic and dissipative processes in the medium have produced negligible effects [22]. With these assumptions, the more familiar equation [1,2,5] for the medium perturbation is recovered, but in this case dissipative effects are properly treated:

$$\begin{aligned} & [\partial_{t_1}^2 - v_0^2 \nabla_\perp^2 - \eta_0 (\frac{4}{3} + r) \partial_{t_1} \nabla_\perp^2] [\partial_{t_1} - (\eta_0 / \rho) \nabla_\perp^2] \delta \rho \\ &= (\gamma - 1) \alpha \nabla_\perp^2 I + \frac{(\gamma - 1)}{\gamma} v_0^2 (\eta_0 / \rho) \nabla_\perp^2 \nabla_\perp^2 \delta \rho. \end{aligned} \quad (17)$$

Equation (17) shows that the optical intensity can induce density variations. In turn, the density variations may alter the intensity through thermal blooming—the density changes induce a refractive-index change that results in focussing or defocussing of the beam. One may write the intensity as

$$I(x, t) = |E_0 + \delta E(x, t)|^2 = I_0 e^{2\chi}, \quad (18)$$

where $I_0 = |E_0|^2$ is the unperturbed laser-beam intensity,

and χ refers to the log-amplitude fluctuations. With this, Eq. (17) may be made linear in the small fluctuations χ :

$$\nabla_\perp^2 I = 2I_0 \nabla_\perp^2 \chi + O(\delta \chi^2). \quad (19)$$

Now, the evolution of the electric field also must be described. The intensity perturbations have been defined; a complementary perturbation of the phase must also be chosen. To do this, use the paraxial equation, with the electric field given by $E(x) = I_0^{1/2} \exp(\chi + i\phi)$. This approach for the optical field is consistent with the Rytov approximation and with that of other authors [13,16,17]. These perturbations of the optical field must then be substituted into the evolution equation for the electric field, given by

$$\begin{aligned} & \left[\partial_z + (1/v_g) \partial_t + \frac{\nabla_\perp^2}{2ik_0} \right] E \\ &= -i(k_0/n_0) \Delta n E - (\alpha'/2) E, \end{aligned} \quad (20)$$

where $\Delta n = (\partial n / \partial \rho)_s \delta \rho + (\partial n / \partial s)_\rho \delta s$ is the induced refractive index variation, $v_g = c/n_0$, c is the speed of light, n_0 is the refractive index of the unperturbed medium, $k_0 = k_{00} n_0$ is the optical wave number in the fluid, and k_{00} is the optical wave number in free space. The quantity $(\partial n / \partial \rho)_s$ is the change in refractive index per unit change in density, at fixed entropy, and is equal to $(n_0 - 1)/\rho_0$ for $n_0 \approx 1$. The change in refractive index with entropy at fixed density is assumed to be zero for the structureless simple fluids we are considering here [24]. Returning to Eq. (20), going to the retarded frame, substituting the Rytov expression for E , equating real and imaginary parts in (20), and linearizing, yields

$$\partial_z \phi - \frac{\nabla_\perp^2}{2k_0} \chi = (k_0/n_0) \Delta n, \quad (21)$$

$$\partial_z \chi + \frac{\nabla_\perp^2}{2k_0} \phi = -\frac{\alpha'}{2}. \quad (22)$$

These last two equations are easily simplified by using Fourier-transform techniques. One defines the Fourier transforms as

$$\chi = \int \exp(-i\mathbf{k} \cdot \mathbf{x}) \delta \chi(\mathbf{k}) dk^2 \quad (23)$$

and

$$\phi = \int \exp(-i\mathbf{k} \cdot \mathbf{x}) \delta \phi(\mathbf{k}) dk^2, \quad (24)$$

where \mathbf{k} denotes the transverse wave number in the following equations, and $\delta \chi$, $\delta \phi$, and δn refer to the Fourier transforms of χ , ϕ , and Δn , respectively. The above inhomogeneous equations then simplify to those corresponding to a harmonic oscillator:

$$\partial_z \delta \phi + \frac{k^2}{2k_0} \delta \chi = (k_0/n_0) \delta n, \quad (25)$$

$$\partial_z \delta \chi - \frac{k^2}{2k_0} \delta \phi = -\frac{\alpha'}{2}. \quad (26)$$

Additional notation for the Fourier components has been dropped here and through the remainder of the paper when no confusion results. In many cases, the direct effect of absorption is unimportant; thus one may ignore the absorption term on the right-hand side. One may also simplify notation by changing the propagation variable to the dimensionless variable $\xi = k^2 z / 2k_0$; one obtains from Eqs. (25) and (26), for each transverse Fourier component,

$$\partial_{\xi} \delta \chi - \delta \phi = 0, \quad (27)$$

$$\partial_{\xi} \delta \phi + \delta \chi = \beta \delta n, \quad (28)$$

where $\beta^{-1} = 2n_0(k/2k_0)^2 \equiv n_0 \beta_0^{-1}$ is proportional to the magnitude squared of the grating vector formed by interference of the laser-beam perturbations with the unperturbed beam. Before proceeding it is worthwhile to mention the utility of the Rytov formalism. The Fourier component of the log-amplitude fluctuation may be expressed as

$$\delta \chi(k) = \frac{1}{2} [E_0^* \delta E(\mathbf{k}) + E_0 \delta E^*(-\mathbf{k})] + O(\delta E)^2,$$

thus this formalism automatically includes the four-photon coupling processes treated by previous authors [9].

To relate the propagation equations to the equations for the medium perturbation, one may substitute the refractive index for the density, assuming $n_0 \approx 1$,

$$\begin{aligned} \delta n(\mathbf{k}) &= \frac{1}{2n_0} \left[\frac{\partial \epsilon_{ii}}{\partial \rho} \right]_s \delta \rho(\mathbf{k}) \\ &= \frac{n_0 - 1}{\rho_0} \delta \rho(\mathbf{k}), \end{aligned} \quad (29)$$

where ϵ_{ii} is a diagonal element of the dielectric tensor for an optically isotropic fluid. Then one obtains the linearized equation of motion

$$\begin{aligned} &[\partial_{t_1}^2 + (v_0|\mathbf{k}|)^2 + \eta_0(\frac{4}{3} + r)|\mathbf{k}|^2 \partial_{t_1}] (\partial_{t_1} + (\eta_0/\epsilon)|\mathbf{k}|^2) \delta n \\ &= -(v_0|\mathbf{k}|)^2 \Gamma_1 I_0 \delta \chi + \frac{(\gamma - 1)}{\gamma} v_0^2 (\eta_0/\epsilon) |\mathbf{k}|^4 \delta n, \end{aligned} \quad (30)$$

where

$$\begin{aligned} \Gamma_1 &= 2(\partial n / \partial \rho)_s \alpha (\alpha_e / c_p) \\ &\approx 2(n_0 - 1)(\gamma - 1) \alpha / \gamma p_0, \end{aligned}$$

so that $\Gamma_1 I_0$ is equal to the optical-path difference per second per meter, induced by thermal blooming in the steady state. Thus $(k_0/n_0)(\Gamma_1 I_0)(2\pi k_0/|\mathbf{k}|^2)$ is the number of radians per second of the thermally induced phase imposed by propagation over a Rayleigh range of the perturbation scale in the steady state. Since our interest is in transient heating of sufficient strength to alter the beam profile, this number is expected to be greater than one in relevant cases. This motivates our choice of normalization of time; one may normalize the time variable to the dimensionless time $\tau_1 = \Gamma_1 I_0 \beta t_1$ and the notation is then simplified by writing

$$\theta(z) = -\mathbf{k} \cdot \mathbf{v}(z) / \Gamma_1 I_0 \beta, \quad (31a)$$

$$\epsilon = (\eta_0/p_r) k^2 / \Gamma_1 I_0 \beta, \quad (31b)$$

$$\mu = v_0 k / \Gamma_1 I_0 \beta. \quad (31c)$$

One then obtains the following dimensionless version of Eq. (30):

$$\begin{aligned} &[\partial_{\tau_1}^2 + \mu^2 + (\frac{4}{3} + r)\epsilon \partial_{\tau_1}] (\partial_{\tau_1} + \epsilon) \delta n \\ &= -\mu^2 \frac{\delta \chi}{\beta} + \frac{\gamma - 1}{\gamma} \mu^2 \epsilon \delta n. \end{aligned} \quad (32)$$

Now we have three dimensionless equations, (27), (28), and (32), in three unknowns, δn , $\delta \phi$, and $\delta \chi$. Two of these unknowns may be eliminated to obtain a simplified equation of motion. To eliminate the phase perturbation $\delta \phi$ one may differentiate Eq. (27) and use Eq. (28) to eliminate $\partial_{\xi} \delta \phi$. One obtains

$$(\partial_{\xi}^2 + 1) \delta \chi = \beta \delta n. \quad (33)$$

Applying the $(\partial_{\xi}^2 + 1)$ operator to both sides of Eq. (32) and substituting $\beta \delta n$ for the differentiated intensity in the resulting equation leads to the following expression, in which simplified notation is used for the explicit form of the differential operator,

$$(\partial_{\xi}^2 + 1) \mathcal{L}_2 \delta n = -\mu^2 \delta n + (\partial_{\xi}^2 + 1) \frac{(\gamma - 1)}{\gamma} \mu^2 \epsilon \delta n. \quad (34a)$$

$$\begin{aligned} &\{[\partial_{\tau} - i\theta(\xi)]^2 + \mu^2 + (\frac{4}{3} + r)\epsilon [\partial_{\tau} - i\theta(\xi)]\} \\ &\quad \times [\partial_{\tau} - i\theta(\xi) + \epsilon] \delta n \equiv \mathcal{L}_2 \delta n, \end{aligned} \quad (34b)$$

This linear partial-differential equation is a significant result of this effort; it may be used to analyze thermal blooming in most heating regimes relevant to laser propagation. To make this equation more relevant to situations of interest, set $\delta n = \delta n_B + \delta n_T$, where δn_B is the blooming contribution, and δn_T is the turbulence contribution. The temporal operator operating on the turbulence contribution yields nearly zero because the turbulence is assumed to obey the frozen-flow hypothesis with diffusion:

$$[\partial_{\tau} - i\theta(\xi) + \epsilon] \delta n_T = 0. \quad (35)$$

Thus Eq. (34) may be simplified to give an inhomogeneous equation for the blooming contribution:

$$\begin{aligned} &\left[(\partial_{\xi}^2 + 1) \left[\mathcal{L}_2 / \mu^2 - \frac{(\gamma - 1)}{\gamma} \epsilon \right] + 1 \right] \delta n_B \\ &= - \left[1 - (\partial_{\xi}^2 + 1) \frac{(\gamma - 1)}{\gamma} \epsilon \right] \delta n_T. \end{aligned} \quad (36)$$

Another simplification is applicable in cases in which the turbulence δn_T is predominantly of low spatial frequency; in such cases

$$|(\partial_{\xi}^2 + 1)[(\gamma - 1)/\gamma] \epsilon \delta n_T| \ll \delta n_T,$$

and the second term on the right-hand side is negligible. This is then the form of the equation used for our analysis. Equation (36) is to be supplemented with Eq.

(33) to obtain the intensity perturbation from the refractive-index perturbation and with Eq. (27) to obtain the phase perturbation from the intensity perturbation. This method allows relatively easy computation of all the dependent variables with closed-form expressions.

The initial conditions remain to be specified. For the blooming-induced refractive-index variations, $\delta n_B = 0$ and all its time derivatives are zero at $t = 0$, for all ξ and all k . This merely restates the assumption that the laser does not heat the medium until it is turned on. At the ξ boundary of the solution region, the value of $\xi = 0$ corresponds to the laser transmitter location. At this boundary the initial conditions are specified and propagate to ξ_{\max} . At $\xi = 0$, $\delta n_B(\xi = 0)$, and $\partial_{\xi} \delta n_B(\xi = 0)$ are determined by the intensity and phase, respectively, of the laser beam. The relations are as follows:

$$\delta n_B(\tau = 0) = \partial_{\tau} \delta n_B(\tau = 0) = \partial_{\tau}^2 \delta n_B(\tau = 0) = 0, \quad (37a)$$

$$\left[\mathcal{L}_2 / \mu^2 - \frac{(\gamma - 1)}{\gamma} \epsilon \right] \delta n \Big|_{\xi=0} = - \frac{\delta \chi}{\beta} \Big|_{\xi=0}, \quad (37b)$$

$$\left[\mathcal{L}_2 / \mu^2 - \frac{(\gamma - 1)}{\gamma} \epsilon \right] (\partial_{\xi} \delta n) \Big|_{\xi=0} = - \frac{\delta \phi}{\beta} \Big|_{\xi=0}. \quad (37c)$$

These equations, (36), (33), (27), and (37), determine the evolution of the heated medium for all times and positions provided the intensity perturbations remain small compared to I_0 . The possibility of compensation for atmospheric turbulence will alter the initial conditions, and this aspect of the problem is treated in Sec. VII.

Before discussing the solutions in detail, important general remarks may be made from the form of the resulting Eqs. (34) and (36), especially regarding scaling of the interaction. The dimensionless scaling parameters give physical insight into the result, and provide useful back-of-the-envelope estimates. These parameters are discussed in the following sections.

III. DISPERSION RELATIONS

The dispersion relations of stimulated thermal scattering have been an important part of the study of stimulated scattering [3,7,9]. In stimulated thermal scattering the intensity that drives the material excitation derives from the interference of the laser beam and a small stimulated wave,

$$I \approx |E_0 \exp[i(\omega t - k_0 z)] + \delta E \exp[i(\omega_1 t - \mathbf{k}_1 \cdot \mathbf{z})]|^2, \quad (38)$$

where \mathbf{z} is the propagation axis, $E_0 \exp[i(\omega t - k_0 z)]$ is the laser-beam electric-field amplitude of optical

frequency ω and optical wave number k_0 , and $\delta E \exp[i(\omega_1 t - \mathbf{k}_1 \cdot \mathbf{z})]$ is the electric field amplitude of a perturbation which may be nearly copropagating or nearly counterpropagating with respect to the laser beam. Hence, $\mathbf{k}_1 = (\pm k_0 + \delta k_z) \hat{\mathbf{z}} + k_1 \hat{\mathbf{e}}_1$. Note in Eq. (38) that we utilize the assumptions of monochromatic radiation and of only one Fourier component of the perturbation. These assumptions apply to this section only; thus in this section only we neglect the important linewidth [21] and four-wave mixing [9] effects. Keeping only terms linear in δE , and equating temporal and spatial frequency components on both sides of Eq. (16a) leads to the amplitude of the medium perturbation. Avoiding the restrictive assumptions after Eq. (16a) and utilizing the corresponding normalizations of Eqs. (31) and of the preceding text leads to a dimensionless dispersion relation for the refractive-index perturbation, which in this case is given by

$$\{ [(i\delta\omega/\mu)^2 + 1 + (\frac{4}{3} + r)\mu(\epsilon/\mu)(i\delta\omega/\mu)](i\delta\omega + \epsilon) - \Phi\epsilon \} \times (i\delta\omega/\Gamma_2 + 1)\delta n = - \frac{\delta E}{\beta E_0}, \quad (39)$$

where

$$I_0 = |E_0|^2, \quad (40a)$$

$$\delta\omega = (\omega_1 - \omega) / \Gamma_1 I_0 \beta, \quad (40b)$$

$$\Gamma_2 = \Gamma / \Gamma_1 I_0 \beta, \quad (40c)$$

$$\Phi = v_0^2 \alpha_e^2 T / \gamma c_p = c_v T \Psi^2 / v_0^2, \quad (40d)$$

$$\theta(z) = -\mathbf{k} \cdot \mathbf{v}(z) / \Gamma_1 I_0 \beta, \quad (40e)$$

$$\epsilon = (\eta_0 / \mu) k^2 / \Gamma_1 I_0 \beta, \quad k = |\mathbf{k}_1 \mp k_0 \hat{\mathbf{z}}|, \quad (40f)$$

$$\mu = v_0 k / \Gamma_1 I_0 \beta. \quad (40g)$$

As in Sec. II the quantity $1/\beta$ is proportional to the squared magnitude of the grating vector formed by interference of the laser-beam perturbations with the unperturbed beam. Thus, in the backward-scattering case,

$$\beta \equiv \beta_0 / n_0 = \frac{1}{2n_0} \left[\left(1 - \frac{1}{2\beta_{10}} \right)^2 + \frac{1}{2\beta_{10}} \right]^{-1} \approx \frac{1}{2n_0},$$

where $1/\beta_{10} = 2(k_1/2k_0)^2$ is the normalized path delay of a beam traveling at an angle $\theta = \mathbf{k}_1/k_0$ with respect to the propagation axis.

Solving for δn and substituting into the linearized, Fourier-transformed, and dimensionalized paraxial equation (20) yields the second equation needed to form the dispersion relation for STBS or STRS:

$$\begin{aligned} & [(\delta k_z/k_0) \pm (\delta\omega/\omega) + 1/\beta_{10} + \alpha/2k_0] \delta E \\ &= (\delta n/n_0) E_0 \\ &= -(\delta E/\beta_0) / \{ [(i\delta\omega/\mu)^2 + 1 + (\frac{4}{3} + r)\mu(\epsilon/\mu)(i\delta\omega/\mu)](i\delta\omega/\epsilon + 1) \epsilon - \Phi\epsilon \} (i\delta\omega/\Gamma_2 + 1), \end{aligned} \quad (41)$$

where $\pm(\delta\omega/\omega)$ refers to copropagation ($-$) or counter-propagation ($+$) of the optical perturbation with respect to the laser beam. The nondimensionalization of Eq. (41) is achieved by division with the optical wave number k_0 ; this contrasts with the nondimensionalization of Sec. II, in which the nondimensionalization is achieved by division with k_0/β_{10} . The present normalization is more suitable for the general case. Equation (41) gives the dispersion relation for stimulated backward thermal scattering as a function of the dimensionless parameters of the problem

$$\theta, \mu, \epsilon, r, \lambda, \Phi, \Gamma_2, \text{ and } \beta_0. \quad (42)$$

With eight dimensionless parameters, a wide range of behavior is possible. For many potential applications, these parameters have typical values. For example, $r \approx 0$, $\theta \approx 0$, $\Phi \approx 0$, $1/\beta_{10} \approx 0$, $\lambda \approx 1$, and $\Gamma_2 > \mu > \epsilon$. In the following, the spatial gain, defined as $\text{Im}(\delta k_z)$, is calculated explicitly in the STBS and STRS limits, and sample gain profiles as a function of frequency are shown. The imaginary part of Eq. (41) therefore provides the gain coefficient for the stimulated process as a function of the pure real frequency offset $\delta\omega$. First consider the STRS limit in which the population decay and the acoustic relaxation rates are much greater than the medium decay rate, $\Gamma_2 \gg \epsilon$, $\mu \gg \epsilon$, and $|\delta\omega/\epsilon| \leq 3$. Using the nominal values given above for the remaining parameters and ignoring terms of order $(\epsilon/\mu)^2$ and order (ϵ/Γ_2) , one finds that the gain $g(\delta\omega)$ per unit length is given by

$$g(\delta\omega) = (k_{00}/\beta)\delta\omega/[\delta\omega^2 + \epsilon'^2] \quad (\text{STRS}), \quad (43)$$

where $\epsilon' = (1 - \Phi)\epsilon$. Note that the gain is positive for frequency-upshifted (anti-Stokes) light, with corresponding absorption for the downshifted light [3]. The gain is at maximum at $\delta\omega = \epsilon'$, with a maximum value of $k_{00}/(2\beta\epsilon')$. The gain linewidth is asymmetric with a full width at half maximum (FWHM) roughly equal to $2(3)^{1/2}\epsilon'$ for STRS with $\epsilon/\mu \ll 1$. In addition to gain, dispersion is also present. The real part of the line corresponds to dispersion that results in phase perturbations and relates to spontaneous molecular scattering [3,6,21,25]. The real part has a peak value of $k_{00}/(\beta\epsilon')$ at $\delta\omega = 0$, with a FWHM of $2\epsilon'$.

Now consider the case in which the same equalities hold but with $|(\delta\omega - \mu)/\epsilon| \leq 3$. Again ignoring terms of order $(\epsilon/\mu)^2$, and now ignoring terms of order (μ/Γ_2) , and of order $(\epsilon/\mu)\Phi/\lambda$,

$$g(\delta\omega) = (k_{00}/\beta)\mu^2(\mu^2 - \delta\omega^2)/[(\mu^2 - \delta\omega^2)^2 + (\epsilon''\delta\omega)^2]\delta\omega \quad (\text{STBS}), \quad (44a)$$

where $\epsilon'' = (\frac{4}{3} + r)\lambda\epsilon$. For STBS, one finds a maximum and a minimum clustered about $\delta\omega = \mu$ and similarly for $\delta\omega = -\mu$. The peak gains occur at $\delta\omega = \pm\mu(1 \mp (\epsilon''/\mu))^{1/2}$. The average absolute value of peak gain and absorption is equal to $k_{00}/(2\beta\epsilon'')$. The FWHM of these gain curves are of the order of ϵ'' . The ratio of the peak STRS gain to the peak STBS gain is roughly equal to $(\frac{4}{3} + r)\lambda/(1 - \Phi)$, i.e., the normalized ratio of total viscosity to total conductivity. The real, dispersive

parts of the Brillouin-shifted wings have a peak value of $k_{00}/(\beta\epsilon'')$ at $\delta\omega = \pm\mu$. The dispersive part of the profile is related to spontaneous scattering, as mentioned above. Through spontaneous scattering this part of the line profile has been observed experimentally [6,25].

To help relate these STBS results to those of previous authors, one may expand the denominator of Eq. (41) in a Taylor series about $\delta\omega = \pm\mu$. Thus the denominator $D(\delta\omega)$ may be written as

$$D(\delta\omega) = a + b(\delta\omega - \mu) + O(\delta\omega - \mu)^2,$$

about $\delta\omega = +\mu$, and similarly for $\delta\omega = -\mu$. If this expansion is used in the small-damping regime in which $(\epsilon'' + \epsilon)/\mu \ll 1$, then the STBS gain profile at $\delta\omega = +\mu$ is approximately

$$g(\delta\omega) = \frac{-(k_{00}/2\beta)(\delta\omega - \mu)}{(\delta\omega - \mu)^2 + (\epsilon''')^2}, \quad (44b)$$

where $\epsilon''' = b/a = (\epsilon'' + \Phi\epsilon)/2$. This then implies a decay rate of

$$\Gamma_h I_0 \beta \epsilon''' = (k^2/2)[\eta_0(\frac{4}{3} + r) + (\gamma - 1)\kappa_T/\rho c_p], \quad (45)$$

in accord with previous authors [6,8,9,25]. Within this approximation, the peak gain is $k_{00}/4\beta\epsilon'''$, with an asymmetric linewidth of width $2(3)^{1/2}\epsilon'''$ (FWHM). Furthermore, the ratio of the peak Rayleigh gain to the peak Brillouin gain is $2\epsilon'''/\epsilon'$ [3].

Corresponding to Eqs. (43) and (44b) for the gain are expressions for the dispersion, which derive from the real part of the dispersion relation. From these expressions for the dispersion, assuming only conductive relaxation (negligible viscosity) in an ideal gas, and assuming the weak-interaction limit $|\delta k_z z| \leq 1$ applies, the Landau-Placzek relation is recovered for the ratio of the spontaneous line intensities [6,25].

The dimensionless thermal diffusion decay rate ϵ is given by (40f) evaluated at the spatial frequency k corresponding to the period of the material grating vector, which is approximately $2k_0$ for backward scattering. Upon expansion of the ratio it is found that $\epsilon/\mu \approx kl$, where l is the mean free path, and $k \approx 2k_0$ for backward scattering. This implies that the damping rate ϵ may exceed the acoustic frequency μ , i.e., $\epsilon/\mu \geq 1$. Thus, the corresponding scattering regime is also of interest. However, based on earlier remarks, the thermodynamic theory underlying our calculations is of questionable validity when ϵ/μ is greater than about 10. Proceeding then with the qualification that $10 \geq \epsilon''/\mu \geq 1$, the gain profile may be rewritten by ignoring terms of order μ/ϵ :

$$g(\delta\omega) = \frac{(k_{00}/\beta)\delta\omega(\mu^2\epsilon''/\epsilon)}{[\delta\omega^2 - (1 - \Phi)\mu^2]^2 + (\epsilon''\delta\omega)^2}. \quad (46)$$

This gain profile has a peak gain of $k_{00}/(2\beta\epsilon')$, similar to the STRS case above; see Eq. (43). The frequency offset at which this peak occurs is $\delta\omega = (1 - \Phi)(\mu/\epsilon'')^2\epsilon''$. The STBS wings have combined with the central line in this limit of large damping; the single peak now has a FWHM of the order of $(\mu/\epsilon'')\mu$. The line is antisymmetric about $\delta\omega = 0$ similar to the STRS profile of Eq. (43) but with an

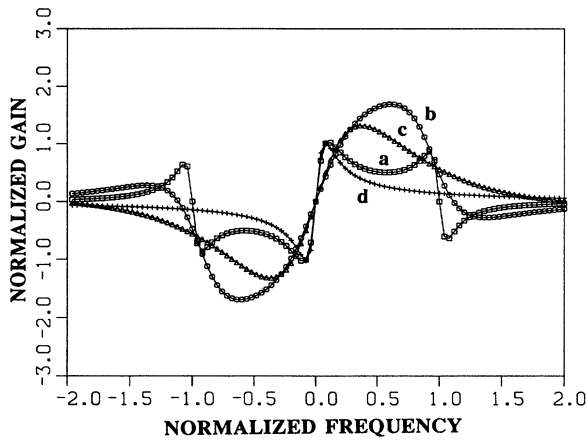


FIG. 1. Normalized gain $\text{Im}[\delta k_z(\delta\omega)]/(k_{00}/2\beta\epsilon)$ vs normalized frequency offset $\delta\omega/\mu$, for $\Gamma_2/\mu=10$, $\Phi=0.001$, $r=0$, $\lambda=1$, and $\epsilon/\mu=0.1$ (squares, a), 0.5 (circles, b), 2 (triangles, c), and 10 (crosses, d).

altered abscissa.

To illustrate the gain profiles, sample gain profiles are computed from Eq. (41) for which the nominal values of the parameters r , Φ , β_1 , λ are used and for $\epsilon/\mu=0.1$, 0.5, 2, and 10. In Fig. 1, a fast population decay and a small ratio Φ is considered: $\Gamma_2/\mu=10$ and $\Phi=0.001$ is assumed. The trends discussed above are illustrated; one observes a gain profile that has distinct gain and absorption peaks clustered at all three lines. Gain occurs for Stokes-shifted light for both Brillouin pairs in agreement with the theoretical and experimental results of other authors [8]. As the viscosity is increased, the individual

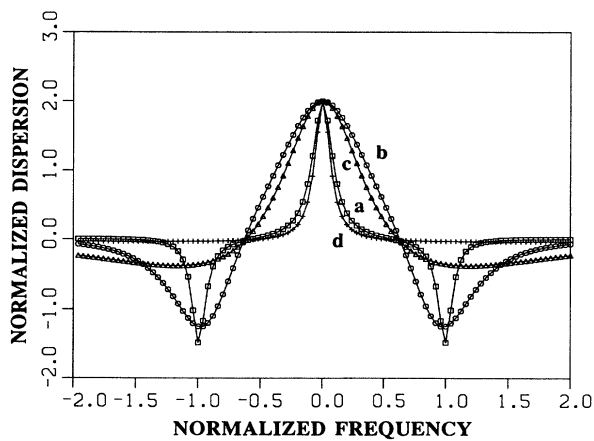


FIG. 2. Normalized dispersion $\text{Re}[\delta k_z(\delta\omega)]/(k_{00}/2\beta\epsilon)$ vs normalized frequency offset $\delta\omega/\mu$, for $\Gamma_2/\mu=10$, $\Phi=0.001$, $r=0$, $\lambda=1$, and $\epsilon/\mu=0.1$ (squares, a), 0.5 (circles, b), 2 (triangles, c), and 10 (crosses, d).

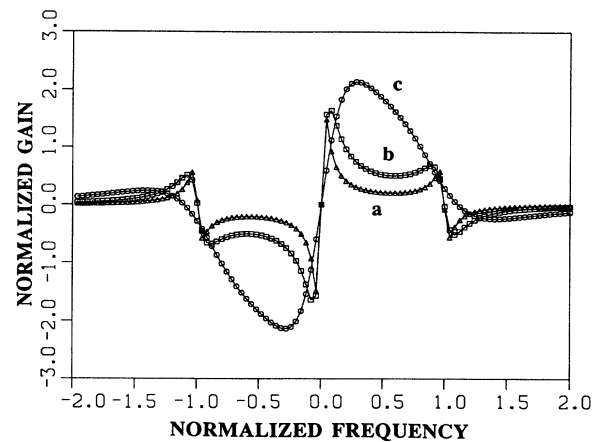


FIG. 3. Normalized gain $\text{Im}[\delta k_z(\delta\omega)]/(k_{00}/2\beta\epsilon)$ vs normalized frequency offset $\delta\omega/\mu$, for $\Gamma_2/\mu=10$, $\Phi=0.4$, $r=0$, $\lambda=1$, and $\epsilon/\mu=0.04$ (squares, a), 0.1 (circles, b), and 0.5 (triangles, c).

lines broaden and merge. These latter cases correspond to the limit in which the grating period becomes comparable to the mean free path. Thus, as discussed above, the validity of the hydrodynamic approximation is questionable for these cases [20]; nonetheless, we include these profiles for completeness and comparison with Eq. (46) above. Note that the peak gain is actually enhanced for intermediate values of the viscosity because the temporal phase relationship between the optical beams and the coherent material oscillation is more favorable for energy transfer. As the viscosity is increased yet further, so that $\epsilon/\mu \geq 1$, the peak and valley of the gain profile move toward line center, in accord with the calculations above. In addition to the gain profile, the dispersion profile

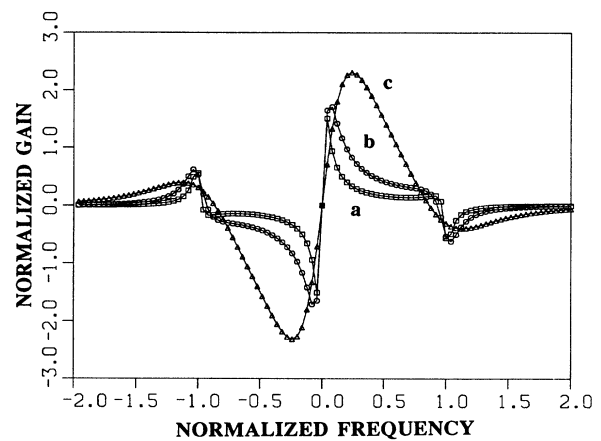


FIG. 4. Normalized gain $\text{Im}[\delta k_z(\delta\omega)]/(k_{00}/2\beta\epsilon)$ vs normalized frequency offset $\delta\omega/\mu$, for $\Gamma_2/\mu=1$, $\Phi=0.4$, $r=0$, $\lambda=1$, and $\epsilon/\mu=0.04$ (squares, a), 0.1 (circles, b), and 0.5 (triangles, c).

$\text{Re}[\delta k_z(\delta\omega)]$ is of interest and is shown in Fig. 2. These lines show the well-known central and Brillouin-shifted profiles, mentioned above, that occur within the hydrodynamic approximation [20].

Figures 3 and 4 show variations in the gain profile. Figure 3 predicts the gain profile with the ratio $\Phi=0.4$, corresponding to a monoatomic ideal gas. Figure 4 additionally includes the effect of a reduced population decay rate for which $\Gamma_2/\mu=1$ is assumed.

These results show qualitative agreement with previously published theoretical and experimental results. Obviously, many real absorbing fluids exhibit behavior that requires analysis beyond that presented here [20].

IV. DIMENSIONLESS SCALING PARAMETERS

From Eqs. (34) or (41) it is evident that there are several dimensionless parameters that are the ratios of several dimensional variables. These dimensional variables define the scales that are physically relevant; the dimensionless parameters define the regime of the scattering. For example, the dimensional time scale $(\Gamma_1 I_0 \beta)^{-1}$ is equal to the time at which π rad of blooming are induced over one Rayleigh range $n_0 D_1^2/\lambda$ of the perturbation scale D_1 . The dimensional propagation distance scale $(k^2/2k_0)^{-1}$ is equal to a Rayleigh range divided by π of the perturbation scale ($D_1=2\pi/k$). That these two scales should be relevant is obvious. The distance scale measures the range over which the phase turns into intensity; intensity fluctuations are what drives the thermal-blooming interaction. The strength of the thermal-blooming interaction in turn becomes important when it is comparable in strength to diffraction. This strength of interaction occurs at the time scale $(\Gamma_1 I_0 \beta)^{-1}$ mentioned above. If this "growth time" is comparable to or greater than the times for amelioration processes such as wind, acoustics, or diffusion, then the thermal-blooming interaction is greatly affected. This is evident from Eq. (34), which involves dimensionless ratios of these time scales.

For example, the dimensionless scale θ is the ratio of the flow-transit time across a perturbation scale, divided by the growth time and multiplied by 2π . Thus if the variation of θ is greater than 1, the heating effect is smeared out over more than one half period of the perturbation, which averages out the induced fluctuation before it further intensifies. Similarly if ϵ is greater than 1, diffusion washes out the blooming-induced phase grating before it can feed back on itself. Another key dimensionless parameter μ is equal to the ratio of the acoustic-transit time divided by the growth time and multiplied by 2π . This last parameter is important at early times at which the acoustic contribution to the heating-induced perturbation is comparable to the steady-state contribution and can result in local focussing. If the heating-growth time is much greater than the acoustic-transit time of the perturbation, then acoustics are not important for the thermal-blooming interaction as may be seen from Eq. (34) (provided the linearized equations remain valid). Thus these dimensionless quantities play an important role in determining the character of the scatter-

ing process, as may be seen from Eq. (34). Furthermore, μ/ϵ and θ/ϵ are proportional to the Reynolds number of the acoustic perturbation and the flow, respectively. θ/μ is the flow Mach number. In addition to the above dimensionless parameters that determine the character of the stimulated scattering, there are dimensionless parameters that characterize the medium—these parameters are r , Φ , and μ . One may refer to Sec. II, or any number of texts discussing fluid mechanics, to find an interpretation of these parameters.

V. SOLUTION PROCEDURE

The above equations may be integrated numerically; however, this procedure for solution of partial differential equations may lead to instabilities and convergence difficulties. To avoid these problems, a useful technique is to apply Laplace or Fourier transforms to either the ξ variable or the τ variable. Since the τ operator is more complicated, more is to be gained by transforming it. Also, since the temporal behavior is believed to have an unstable (not periodic) behavior, the Laplace transform appears more suitable than the Fourier transform [5]. Performing the Laplace transform with respect to τ_1 in Eq. (36) leads to

$$\begin{aligned} & ((\partial_\xi^2 + 1) \{ [(s/\mu)^2 + 1 + (\frac{4}{3} + r)\mu(\epsilon/\mu^2)s](s + \epsilon) \\ & - [(\gamma - 1)/\gamma]\epsilon\} + 1) \delta n_B(k, \xi, s) \\ & = -\delta n_T(k, \xi, t=0)/(s + \epsilon), \quad (47) \end{aligned}$$

where s is the transform variable. To put this expression into a more obvious form, define a new variable $G(s)$ associated with the rate of change of the perturbation along the propagation axis. This new variable is defined so that it clearly reduces to the correct no-heating value in the corresponding limit. Thus,

$$\begin{aligned} 1/[G(s)^2 - 1] & \equiv [(s/\mu)^2 + 1 \\ & + (\frac{4}{3} + r)\mu(\epsilon/\mu^2)s](s + \epsilon) \\ & - [(\gamma - 1)/\gamma]\epsilon. \quad (48) \end{aligned}$$

Then Eq. (47) may be rewritten as

$$[\partial_\xi^2 + G(s)^2] \delta n_B = -\delta n_T(k, \xi, 0)[G(s)^2 - 1]/(s + \epsilon). \quad (49)$$

This equation may be solved immediately:

$$\begin{aligned} \delta n_B & = A \cos[G(s)\xi] + B \sin[G(s)\xi] \\ & - \int_0^\xi d\xi' \delta n_T(\xi', 0)[G(s)^2 - 1] \\ & \times \frac{\sin[G(s)(\xi - \xi')]}{G(s)(s + \epsilon)}. \quad (50a) \end{aligned}$$

The constants A and B are determined by the initial conditions at $\xi=0$. From Eqs. (37), one obtains

$$\delta n_B(k, \xi=0, s) = -\delta\chi(k, \xi=0, s)[G(s)^2 - 1]/\beta = A, \quad (50b)$$

$$\begin{aligned}\partial_{\xi}\delta n_B(k, \xi=0, s) &= -\delta\phi(k, \xi=0, s)[G(s)^2-1]/\beta \\ &= BG(s).\end{aligned}\quad (50c)$$

Equations (50a)–(50c) are used to obtain the explicit expression for the heating-induced refractive-index variations.

For the intensity perturbation, one may take the Laplace transform of Eq. (32) and solve

$$\delta\chi(k, \xi, s) = -\beta\delta n_B/[G(s)^2-1]. \quad (51a)$$

This last expression seems to ignore turbulence-only induced scintillations; this is not the case because as the heating rate tends to zero, both δn_B and $G(s)^2-1$ tend to zero also. Thus this expression is not defined in that limit. However, it will be seen that turbulence-induced scintillation is included at time zero. A similar equation for $\delta\phi$ is derivable from Eq. (27):

$$\delta\phi(k, \xi, s) = \partial_{\xi}\delta\chi = -\beta(\partial_{\xi}\delta n_B)/[G(s)^2-1]. \quad (51b)$$

Thus one may write the following for the spatial-temporal evolution of the Fourier components of the intensity and phase (conduction of turbulent variations are neglected):

$$\begin{aligned}\delta\chi(k, \xi, s) &= \delta\chi(k, \xi=0, s) \cos[G(s)\xi] \\ &+ \delta\phi(k, \xi=0, s) \sin[G(s)\xi]/G(s) \\ &+ \beta \int_0^{\xi} d\xi' \sin[G(s)(\xi-\xi')] \\ &\quad \times \delta n_T(\xi', 0)/G(s)s,\end{aligned}\quad (52a)$$

$$\begin{aligned}\delta\phi(k, \xi, s) &= -\delta\chi(k, \xi=0, s)G(s) \sin[G(s)\xi] \\ &+ \delta\phi(k, \xi=0, s) \cos[G(s)\xi] \\ &+ \beta \int_0^{\xi} d\xi' \cos[G(s)(\xi-\xi')] \\ &\quad \times \delta n_T(\xi', 0)/s.\end{aligned}\quad (52b)$$

Note that Eq. (52a) has a turbulence-only induced scintillation term that remains as the heating rate tends to zero and $G(s)$ tends to 1. Also note that the initial conditions at $\xi=0$ play an important role. Further, note that the turbulence-induced refractive-index fluctuations are a random process, thus so too are the phase and intensity.

The second moments $\langle |\delta\chi(k, \xi, \tau)|^2 \rangle$ and $\langle |\delta\phi(k, \xi, \tau)|^2 \rangle$ of the above random variables are of interest. In the case in which the turbulence is uncompensated, the boundary conditions are relatively simple. In many instances, however, the laser may be precompensated for the medium aberrations in order to more effectively propagate the laser beam. This more complicated case is treated in Sec. VII.

It is assumed that the phase and intensity fluctuations on the transmitted beam arise from atmospheric turbulence, the laser, and from optical imperfections. These errors are assumed independent from one spatial frequency to the next. Also assumed independent are the phase and intensity perturbations for a given spatial frequency. The aberrations are assumed constant over the duration of the pulse and are band-limited white out to spatial frequency k_c , i.e.,

$$\langle |\delta\chi(k, 0, s)|^2 \rangle = \begin{cases} \langle |\delta\chi_0|^2 \rangle / \pi k_c^2 s^2 & \text{for } |\mathbf{k}| < k_c \\ 0 & \text{otherwise,} \end{cases} \quad (53a)$$

$$\langle |\delta\phi(k, 0, s)|^2 \rangle = \begin{cases} \langle |\delta\phi_0|^2 \rangle / \pi k_c^2 s^2 & \text{for } |\mathbf{k}| < k_c \\ 0 & \text{otherwise.} \end{cases} \quad (53b)$$

Finally, the turbulence-induced refractive index is assumed to obey a von Kármán spectrum:

$$\langle \delta n_T(k, \xi, 0) \delta n_T^*(k_1, \xi_1, 0) \rangle = 0.033 C_n^2 (k_{0T}^2 + k^2)^{-11/6} \exp \left[- \left[\frac{k}{k_{in}} \right]^2 \right] \delta(\xi_1 - \xi) \left[\frac{k^2}{2k_0} \right] \delta(k_1 - k) \left[\frac{\pi}{2} \right], \quad (54)$$

where C_n is the structure function of turbulence-induced refractive-index variations, k_{0T} is the outer scale of turbulence, and k_{in} is the inner scale [17]. The δ function in ξ as well as the last factor of $\pi/2$ is a consequence of the Markov approximation [17]. The third-to-last factor of Eq. (54) is present because the δ function is a function of ξ and not z . Thus taking the second moments of interest, one finds the following expressions:

$$\begin{aligned}\langle |\delta\chi(k, \xi, \tau)|^2 \rangle &= \frac{\langle |\delta\chi_0|^2 \rangle}{\pi k_c^2} \left| \frac{1}{2\pi} \int_{\epsilon-i\infty}^{\epsilon+i\infty} ds \frac{1}{s} \cos[G(s)\xi] e^{s\tau} \right|^2 + \frac{\langle |\delta\phi_0|^2 \rangle}{\pi k_c^2} \left| \frac{1}{2\pi} \int_{\epsilon-i\infty}^{\epsilon+i\infty} ds \frac{1}{s} \frac{\sin[G(s)\xi]}{G(s)} e^{s\tau} \right|^2 \\ &+ \beta^2 \left[\frac{\pi}{4} \frac{k^2}{k_0} \right] \{ 0.033 (k_{0T}^2 + k^2)^{-11/6} \exp[-(k/k_{in})^2] \} \\ &\quad \times \left| \int_0^{\xi} d\xi' C_n^2 \left[\frac{1}{2\pi} \int_{\epsilon-i\infty}^{\epsilon+i\infty} ds e^{s\tau} \frac{1}{sG(s)} \sin[G(s)(\xi-\xi')] \right] \right|^2,\end{aligned}\quad (55)$$

$$\begin{aligned}
\langle |\delta\phi(k, \xi, \tau)|^2 \rangle = & \frac{\langle |\delta\chi_0|^2 \rangle}{\pi k_c^2} \left| \frac{1}{2\pi} \int_{\epsilon-i\infty}^{\epsilon+i\infty} ds \frac{1}{s} G(s) \sin[G(s)\xi] e^{s\tau} \right|^2 + \frac{\langle |\delta\phi_0|^2 \rangle}{\pi k_c^2} \left| \frac{1}{2\pi} \int_{\epsilon-1\infty}^{\epsilon+1\infty} ds \frac{1}{s} \cos[G(s)\xi] e^{s\tau} \right|^2 \\
& + \beta^2 \left[\frac{\pi}{4} \frac{k^2}{k_0} \right] \{0.033(k_{0T}^2 + k^2)^{-11/6} \exp[-(k/k_{in})^2]\} \\
& \times \int_0^\xi d\xi' C_n^2 \left| \frac{1}{2\pi} \int_{\epsilon-i\infty}^{\epsilon+i\infty} ds \frac{1}{s} \cos[G(s)(\xi - \xi')] e^{s\tau} \right|^2.
\end{aligned} \tag{56}$$

The last term in Eqs. (55) and (56) yields the turbulence-only contribution for the blooming. In the limit as the heating rate goes to zero, $G(s)$ tends to 1, and in this limit the first two terms tend to the diffraction-only values, as does the turbulence contribution. The above are the equations used to compute the power spectral density of the phase and intensity and thus the structure functions and the far-field laser irradiance profile.

VI. COMPARISON OF ANALYTIC THEORY AND NUMERICAL SIMULATION

In order to test the applicability of the linearized analytic theory described in the previous section, results from this theory were compared to output from a wave-optics-propagation computer program that includes the nonlinearity of the optical intensity in Eq. (16). This program models the density perturbations using Eq. (16a), utilizing fast-Fourier-transform techniques for spatial variations and numerical integrations for the temporal variations. The first comparison involved the calculation of the power spectra of the variance of the phase and intensity aberrations as a function of time. For this calculation, it was assumed that the input conditions consisted of random small-scale intensity aberrations imposed on a plane wave. These perturbations were formed from band-limited Gaussian white noise with spatial scales between 0.5 and 10.0 cm and had a total log-amplitude variance of 0.000 25. For larger variances, difficulties arose in calculating the power spectra of the phase, since the severe small-scale thermal blooming present for large input aberrations induced large phase differences between adjacent grid points in our computer simulation that resulted in failure of our phase-reconstruction routine. Increasing the number of grid points to eliminate this problem for large variances would have been computationally prohibitive. It should be noted that the behavior of the far-field spot is not subject to this limitation since it does not involve phase reconstruction; however, grid resolution is still an issue.

For the power spectra comparisons, the absorption and laser intensity were adjusted to yield an average heating rate of $\sim 10^6$ rad/sec, a rate chosen to provide significant thermal blooming within a 10 μ sec pulse. A laser wavelength of 2.8 μ m was used for this comparison. The propagation distance was 5 m, with a corresponding diffraction zone of 0.37 cm over the path length. The simulated path comprised air at standard temperature and pressure, with 17 Torr of chloroethane as the absorb-

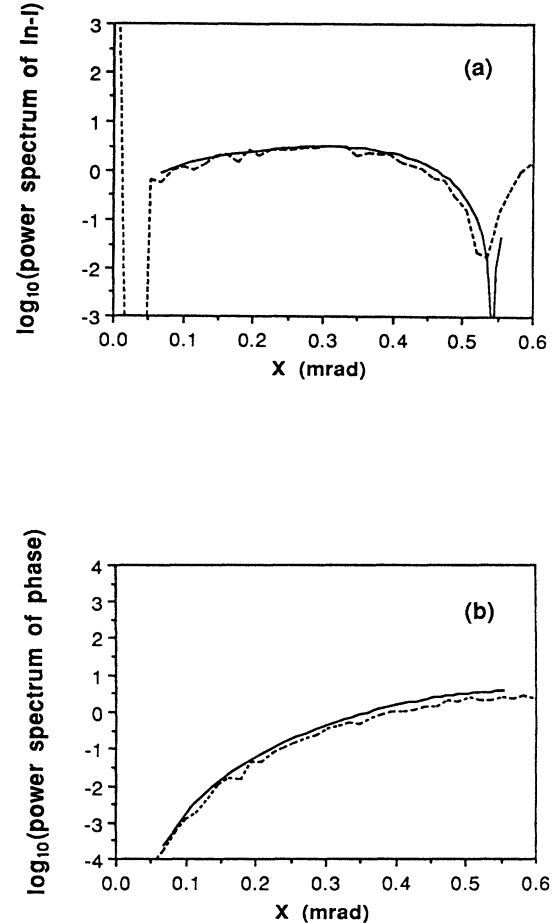


FIG. 5. (a) Frequency dependence of the logarithm (base 10) of the ring-averaged power spectral density of the natural logarithm of the relative intensity perturbations, equal to $\log_{10}\{\pi\langle[\delta\chi(x, z_{\max})]^2\rangle/\langle[\delta\chi(x, z=0)]^2\rangle\}$, before blooming occurs. z_{\max} denotes the end of the cell, x is the scattering angle equal to λ/D , where λ is the optical wavelength, and D is the perturbation scale. The initial profile comprises Gaussian random intensity modulation of total variance $\langle(\delta I/I_0)^2\rangle=0.001$, with a band-limited white-noise power spectrum. Solid and dashed curves are analytical and numerical results, respectively. (b) Frequency dependence of the logarithm (base 10) of the ring-averaged power spectral density of the phase perturbations, equal to $\log_{10}\{\pi\langle[\delta\phi(x, z_{\max})]^2\rangle/\langle[\delta\chi(x, z=0)]^2\rangle\}$ before blooming occurs at end of cell. Solid and dashed curves are analytical and numerical results, respectively.

ing contaminant. Results from these runs are presented in Figs. 5 and 6. Figure 5 shows output from the beginning of the simulation and Fig. 6 presents the output at 10 μsec into the pulse. In Fig. 5, the two minima in the power spectrum of the variance of the intensity indicate the range of the band-limited noise. By 10 μsec , the minimum at the larger angle has shifted to a lower spatial frequency reflecting the presence of acoustic relaxation at smaller scales. Similar trends are seen in the plots of the phase variance. For both time slices, agreement between the linear analytic theory and the nonlinear computer simulation is excellent, within the frequency band for which both approaches are valid. This leads us to conclude that the linear theory contains most of the important physics of transient thermal blooming, and that nonlinear effects are unimportant for conditions of interest. This is consistent with results obtained for steady-state thermal blooming in a separate theoretical effort [13].

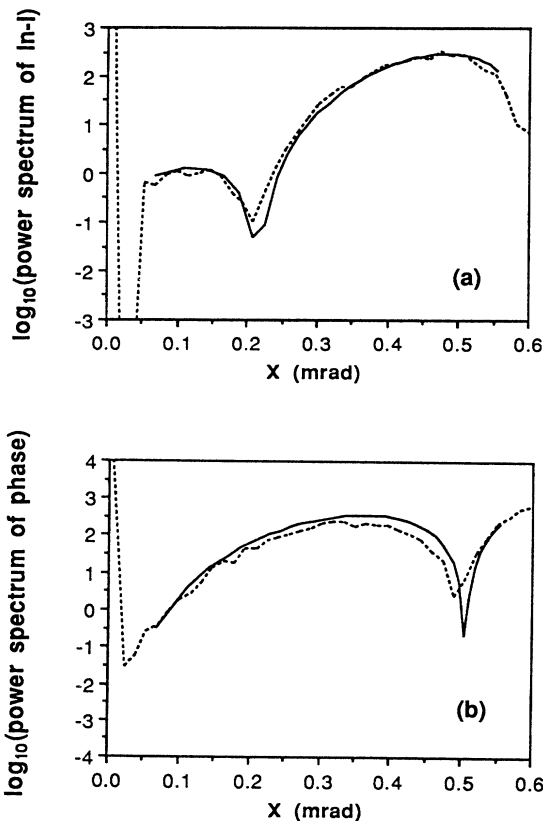


FIG. 6. (a) Frequency dependence of the logarithm (base 10) of the ring-averaged power spectral density of the logarithm of the relative intensity perturbations after 10 μsec of irradiation at end of cell. The time dependence of the minimum in the variance is due to acoustic relaxation of small spatial scales. Solid and dashed curves are analytical and numerical results, respectively. (b) Frequency dependence of the logarithm (base 10) of the ring-averaged power spectral density of the phase perturbations after 10 μsec of irradiation at end of cell. Solid and dashed curves are analytical and numerical results, respectively.

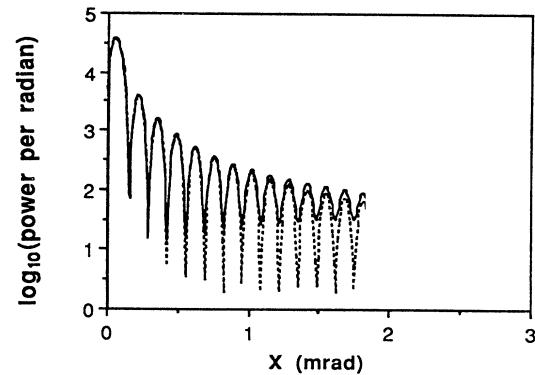


FIG. 7. Angular dependence of the logarithm of the ring-integrated far-field laser-irradiance profile prior to blooming. The structure in the profile are ordinary diffraction rings. $x = d/L$, where d is displacement from focus, and L is the lens focal length. Solid and dashed curves are analytical and numerical results, respectively.

Figures 7–9 contain results from a finite-beam calculation. The following input conditions are applicable to this calculation. A laser beam at 10.6 μm with a flat-top intensity profile and a beam diameter of 8 cm passed through a cell 5 m in length. The laser fluence was adjusted so that 10 rad of blooming occurred in 10 μsec ; air with an absorbing contaminant was again the heated fluid. Band-limited Gaussian noise was used to model the initial intensity aberrations, with scale sizes between 0.5 and 8 cm, and with a variance of 1%.

Plotted in Figs. 7–9 are time-resolved results for the angular dependence of the laser far-field spot. Figure 7 presents a plot of the far-field profile of the laser beam before acoustic relaxation. The profile is ring integrated about the point of peak intensity. The structure of the profile is due to the finite beam size. The minimum occurring near 10^{-4} rad corresponds to the angular loca-

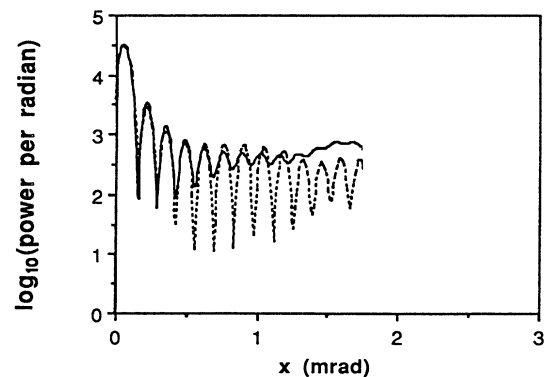


FIG. 8. Angular dependence of the logarithm of the ring-integrated far-field laser-irradiance profile after 10 μsec of medium irradiation. Solid and dashed curves are analytical and numerical results, respectively.

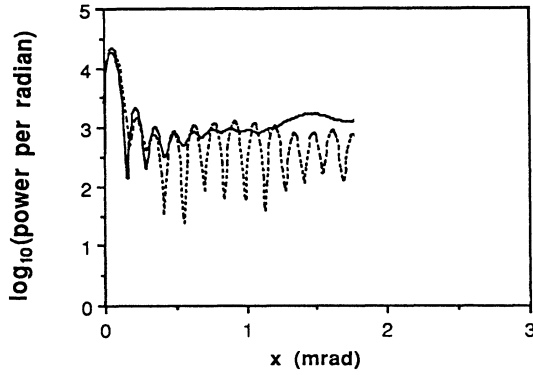


FIG. 9. Angular dependence of the logarithm of the ring-integrated far-field laser-irradiance profile after 15 μsec of medium irradiation. Note a 55% reduction in the peak far-field irradiance. Solid and dashed curves are analytical and numerical results, respectively.

tion of the edge of the central lobe of the far-field spot. After 10 μsec of laser operation, the power at large angles, which correspond to small spatial scales in the near field, has increased significantly. This is shown in Fig. 8. After 15 μsec , the signal at wide angles has increased by more than an order of magnitude over the unblomed values, and the Strehl ratio has fallen by more than 50% as shown in Fig. 9.

Agreement between analytic theory and computer simulation for the finite beam again seems quite good over the common range of validity. Some discrepancies may occur in this case because the analytic theory presented here does not treat beam-edge effects, though such a treatment is possible within the Rytov approximation and perhaps with a generalized Huygens-Fresnel approach [26]. However, such treatments account for whole-beam effects only with greatly increased computational complexity. That whole-beam effects play a role is evident from the altered shape of the central lobe.

The results from the comparison between analytic theory and code simulation indicate that both methods, developed independently, accurately model the physics of transient thermal blooming. This approach rules out the presence of both numerical instabilities and significant convergence errors in the simulation. This approach also validates the scaling relations obtained from the linearized theory.

VII. PHASE-COMPENSATION INSTABILITIES

The previous sections show that aberrations will occur as a consequence of heating of a medium by a laser beam possessing transverse coherence. To mitigate these laser-beam aberrations, one might propose measurement of these (phase) aberrations, and subsequent precompensation of the beam in order to obtain good beam quality after traversal of the heated medium. Unfortunately, the following calculations show that precompensation of phase only will result in instabilities that will intensify the medium perturbations. On the other hand, several authors have shown that phase and amplitude compensation may work [13–15]. Unfortunately, such amplitude compensation has practical difficulties; hence the following considers phase-only compensation [13–15,27].

With phase-only compensation, the initial phase at $\xi=0$ is a function of the sensed phase. For the sake of our analysis, it will be assumed the Fourier components of the phase are corrected, and therefore a function of the measured phase

$$\delta\phi(k, \xi=0, s) = c(k, s)\phi_m(k, s) + \delta\phi_0(k, s), \quad (57)$$

where $c(k, s)$ is a proportionality constant, equal to -1 for perfect compensation, and tending to zero outside the spatial frequency cutoff k_c and the temporal frequency cutoff $\text{Im}(s_c)$. $\delta\phi_0$ is a random compensation error, and ϕ_m is the measured phase, which is equal to the phase of a counterpropagating beacon wave that samples the turbulence. From Eqs. (27) and (28),

$$\begin{aligned} \phi_m(k, s) = & -\delta\chi_b(k, \xi=\xi_{\max}, s) \sin(\xi_{\max}) \\ & + \delta\phi_b(k, \xi=\xi_{\max}, s) \cos(\xi_{\max}) \\ & + \beta \int_0^{\xi_{\max}} d\xi' \cos(\xi') \left[\frac{\delta n_T(k, \xi', 0)}{s} \right. \\ & \left. + \delta n_B(k, \xi', s) \right]. \quad (58) \end{aligned}$$

At this point the counterpropagating beacon's initial intensity and phase $\delta\chi_b(k, \xi=\xi_{\max}, s)$ and $\delta\phi_b(k, \xi=\xi_{\max}, s)$, respectively, are set to zero so that the returning wave is unaberrated if perfectly compensated. Note that the beacon phase at $\xi=0$ obviously depends on the blooming disturbance, and from Eq. (50), the beacon phase in turn depends on the initial phase $\phi(k, \xi=0, s)$ set by phase compensation. Substituting from Eqs. (50) for δn_B in Eq. (58) yields the expression for the compensating phase in terms of known quantities

$$\begin{aligned} \delta\phi(k, \xi=0, s) & \left[1 + c(k, s) \int_0^{\xi_{\max}} d\xi' \cos(\xi') \frac{\sin[G(s)\xi']}{G(s)} [G(s)^2 - 1] \right] \\ & = +c(k, s)\beta \int_0^{\xi_{\max}} d\xi' \left[\cos(\xi') \frac{\delta n_T(k, \xi', 0)}{s} \right] + \delta\phi_0(k, s) \\ & - c(k, s)\delta\chi(k, \xi=0, s) \int_0^{\xi_{\max}} d\xi' \cos(\xi') \cos[G(s)\xi'] [G(s)^2 - 1] \\ & - \beta c(k, s) \int_0^{\xi_{\max}} d\xi' \cos(\xi') \int_0^{\xi'} d\xi'' \delta n_T(\xi'', 0) [G(s)^2 - 1] \sin[G(s)(\xi' - \xi'')] / G(s) s. \quad (59) \end{aligned}$$

The term in large parentheses on the left-hand side of Eq. (59) will be denoted $Q(s)$. Dividing (59) by $Q(s)$ and substituting $\delta\phi(k, \xi=0, s)$ into Eqs. (51) then yields the phase and intensity errors $\delta\chi(k, \xi, s)$ and $\delta\phi(k, \xi, s)$, with compensation. Equations (55) and (56) are then modified accordingly. Written in this form, the equations are substantially more complicated with compensation—multiple integrals such as those present in the last term of (59) make the numerical evaluation significantly more difficult. Nevertheless, useful information may be gained from considering the pole introduced by the term $Q(s)$. This pole leads to a compensation instability described by previous authors [14,27]. The resulting equation gives a spectrum of temporal gains that agrees exactly with Ref. [14], despite the very different form of the integral equation for the pole locations, given by s such that $Q(s)=0$. Because this equation involves an integral along the propagation path that implicitly includes transverse flow, this form for $Q(s)$ has a distinct advantage in its generalization to random wind variations along the optical path. Using this formulation allows the gain to be estimated as a function of the wind profile; such a calculation is beyond the scope of this paper.

VIII. CONCLUSIONS

The above results obtained through two different methods suggest a number of important conclusions. First, one observes that the linearized theory does prove adequate for analysis of the STBS regime and that the numerical simulation is stable and convergent. This may be seen in the excellent agreement between the two approaches. Furthermore, the agreement shows that the nonlinearities modeled by the full simulation are not essential in cases of interest, despite the substantial Strehl reduction.

Second, the results of Fig. 6 indicate that the simple t^3 analysis is not appropriate; such an analysis would lead to no amplification of the intensity perturbations and to an amplification of phase proportional to the square of the angular frequency. As may be seen from a comparison of Figs. 5 and 6, one does not observe these features associated with the simple analysis, i.e., a t^6 time dependence and a k^4 spatial frequency dependence of the power spectral density of the perturbations. Third, the modeling predicts that much of the energy is redistributed in a broad region about focus. This wide-angle scatter is

sometimes described as “lost energy” by other authors for related phenomena [12].

The efforts of this work have been directed to an analytically tractable description of laser heating. Such a description provides closed-form integrals for the perturbations of the laser beam and the medium. These integrals complement numerical techniques [28] for which the convergence and resolution requirements are not well defined. This is especially true for transient laser heating, in which fine temporal and spatial scales, physical instabilities, and backward scattering may be present. The detailed mathematical description given here also shows that STRS and STBS differ from other stimulated scattering processes such as Raman and Brillouin scattering. Heating-induced scattering has most of its gain at higher frequencies relative to the pump beam, unlike both Raman and Brillouin scattering [3]. Thermal scattering is intrinsically a scalar interaction; this characteristic contrasts with that of Raman scattering, for which higher-order symmetries may contribute [29].

The analysis also derives the linearized equations in dimensionless form. These equations then provide useful scaling information. The dimensionless scaling parameters allow quick estimates of the importance of various physical effects and admit straightforward physical explanations. The effects of acoustic, diffusive, and convective energy transport are included in the model. The model is simply extended to cases involving turbulence, active precompensation, and exothermic laser-induced chemical reactions. These effects might be important for applications involving atmospheric propagation or intrapulse phase conjugation of laser-beam aberrations. The expressions obtained for these extensions yield results that concur with other authors in the nonacoustic regime. These comparisons and those above suggest that our theory successfully extends the linearized theory for coupled optical-entropy perturbations (STRS) at late times to optical-acoustic waves (STBS) at early times.

ACKNOWLEDGMENTS

The authors wish to acknowledge Dr. Gerry Quigley of Los Alamos National Laboratory for providing examples of lasers and absorption cells, and Susan Lynch for programming assistance. The authors acknowledge critical contributions from the late Dave Korff in this work.

-
- [1] J. L. Walsh and P. B. Ulrich, in *Laser Propagation in the Atmosphere*, edited by J. W. Strohbehn (Springer-Verlag, Berlin, 1978).
 - [2] J. Wallace and M. Camac, *J. Opt. Soc. Am.* **60**, 1587 (1970).
 - [3] R. M. Herman, and M. A. Gray, *Phys. Rev. Lett.* **19**, 824 (1967); D. H. Rank, C. W. Cho, N. D. Foltz, and T. A. Wiggins, *Phys. Rev. Lett.* **19**, 828 (1967).
 - [4] D. H. Chambers, T. J. Karr, J. R. Morris, P. G. Cramer, J. A. Viecelli, and A. K. Gautesen, *Phys. Rev. A* **41**, 6982 (1990).
 - [5] J. J. Bernard, *Appl. Opt.* **28**, 438 (1989).
 - [6] I. P. Batra, R. H. Enns, and D. Pohl, *Phys. Status Solidi* **48**, 11 (1971).
 - [7] K. A. Brueckner and S. Jorna, *Phys. Rev.* **164**, 182 (1967).
 - [8] D. Pohl and W. Kaiser, *Phys. Rev. B* **1**, 31 (1970); W. Kaiser and M. Maier, in *Laser Handbook*, edited by F. T. Arrechi and E. O. Schulz-Dubois (North-Holland, Amsterdam, 1972), p. 1111.
 - [9] N. M. Kroll and P. L. Kelley, *Phys. Rev. A* **4**, 763 (1971).
 - [10] V. V. Vorob'ev and V. V. Shemetov, *Izv. Vyssh. Uchebn. Zaved. Radiofiz.* **21**, 1610 (1978) [*Sov. Radiophys.* **33**, 1119 (1979)]; B. S. Agrovskii, A. S. Gurvich, V. A. Myakinin, and V. V. Vorob'ev, *J. Opt. Soc. Am. A* **12**, 2304

- (1985).
- [11] R. J. Briggs, Lawrence Livermore National Laboratory, Report No. UCID-21118, 1987 (unpublished).
- [12] A. Flusberg, T. Cronburg, D. Korff, and G. Theophanis, in *Proceedings of the International Conference on Lasers '83*, edited by K. M. Corcoran, D. M. Sullivan, and W. C. Stwalley (STS, McLean, VA, 1984); A. Flusberg and D. Korff, *J. Opt. Soc. Am. B* **3**, 1338 (1986). See also K. S. Gochelashvili, I. V. Chasei, and V. I. Shishov, *Kvant. Elektron. (Moscow)* **7**, 2077 (1980) [*Sov. J. Quantum Electron.* **10**, 1207 (1980)].
- [13] R. Myers, D. Korff, and B. Hatfield, private communication.
- [14] T. J. Karr, *J. Opt. Soc. Am. A* **6**, 1038 (1989).
- [15] J. R. Morris, *J. Opt. Soc. Am.* **6**, 1859 (1989).
- [16] T. J. Karr, J. R. Morris, D. H. Chambers, J. A. Viecelli, and P. G. Kramer, *J. Opt. Soc. Am. B* **7**, 1103 (1990).
- [17] V. I. Tatarski, *The Effects of the Turbulent Atmosphere on Wave Propagation* (National Technical Information Service, Springfield, VA, 1971); see also J. W. Strohbehn, in *Laser Propagation in the Atmosphere* (Ref. 1), p. 51.
- [18] R. Szeto and D. Fried, private communication.
- [19] Frederick G. Gebhardt, *Appl. Opt.* **15**, 1476 (1976).
- [20] L. I. Mandel'shtam and M. A. Leontovich, *Zh. Eksp. Teor. Fiz.* **7**, 438 (1937); see also M. Leontovich, *J. Phys. (Moscow)* **4**, 499 (1941).
- [21] M. A. Gray and R. M. Herman, *Phys. Rev.* **181**, 374 (1969).
- [22] D. R. Dietz, C. W. Cho, and T. A. Wiggins, *Phys. Rev.* **182**, 259 (1969).
- [23] A. L. Fetter and J. D. Walecka, *Theoretical Mechanics of Particles and Continua* (McGraw-Hill, New York, 1980), Chap. 12.
- [24] I. L. Fabelinskii, *Molecular Scattering of Light* (Plenum, New York, 1968) pp. 34–36.
- [25] I. L. Fabelinskii, *Molecular Scattering of Light* (Ref. 24), pp. 81–96, 360.
- [26] H. T. Yura, *Appl. Opt.* **11**, 1399 (1972).
- [27] L. C. Bradley and J. Herrmann, *Appl. Opt.* **13**, 331 (1974).
- [28] J. A. Fleck, J. R. Morris, and M. D. Feit, *Appl. Phys.* **10**, 129 (1976), **14**, 99 (1977).
- [29] R. B. Holmes and A. Flusberg, *Phys. Rev. A* **37**, 1588 (1988).